



HAL
open science

Why and how In composition fluctuations appear in InGaN?

Jean-Yves Duboz, Wanda Isnard, Jesus Zúñiga-Pérez, Jeans Massies

► **To cite this version:**

Jean-Yves Duboz, Wanda Isnard, Jesus Zúñiga-Pérez, Jeans Massies. Why and how In composition fluctuations appear in InGaN?. *Journal of Crystal Growth*, 2023, 603, pp.127033. 10.1016/j.jcrysro.2022.127033 . hal-03902241

HAL Id: hal-03902241

<https://hal.science/hal-03902241>

Submitted on 16 Dec 2022

HAL is a multi-disciplinary open access archive for the deposit and dissemination of scientific research documents, whether they are published or not. The documents may come from teaching and research institutions in France or abroad, or from public or private research centers.

L'archive ouverte pluridisciplinaire **HAL**, est destinée au dépôt et à la diffusion de documents scientifiques de niveau recherche, publiés ou non, émanant des établissements d'enseignement et de recherche français ou étrangers, des laboratoires publics ou privés.

Why and how In composition fluctuations appear in InGaN ?

Jean-Yves Duboz^{a)}, Wanda Isnard, Jesus Zuniga-Perez, and Jean Massies

Université Côte d'Azur, CNRS, CRHEA, 06560, Valbonne, France

a) Corresponding author electronic mail : jyd@crhea.cnrs.fr

Abstract:

We modeled by kinetic Monte Carlo simulations the growth of InGaN alloys on perfectly oriented and misoriented GaN surfaces. As the growth temperature increases, we show that two phenomena occur: composition pulling along the growth direction and lateral indium rich cluster formation. We show that both phenomena have the same origin, strain, and that temperature enables these phenomena to manifest themselves in measurable quantities. Indeed, there is a continuous transition as a function of growth temperature between statistical alloys, described by a binomial distribution law, and heterogeneous layers with indium rich clusters occurring at higher growth temperatures. We quantify this transition by introducing a cluster index based on the In and Ga atom spatial distribution. We show that this cluster index increases above a given temperature, while at low temperature and, in thin layers, it is determined by surface roughness and the associated In fluctuations. Composition pulling can be observed on a larger temperature range. Composition fluctuations are thus caused by strain, and permitted by In mobility at the surface during growth at sufficiently high temperature.

Keywords

A1. Fundamental Aspects: Computer simulation

A1. Fundamental Aspects: Surface processes

A1. Fundamental Aspects: Growth models

A1. Fundamental Aspects: Nanostructures

B1. Materials by Type: Nitrides

B2. Materials by Property Class: Semiconducting III-V materials

1- Introduction

Lighting has been revolutionized in the last 20 years by the introduction of nitride based Light Emitting Diodes (LEDs). The active region of these LEDs is made of one or a few InGaN quantum wells. As these nitride layers are grown on foreign substrates, generally sapphire, the related lattice mismatch leads to a large density of dislocations, initially in the 10^{10} cm^{-2} , and currently in the 10^8 cm^{-2} ranges. While other semiconductors would fail emitting light with such dislocation densities, a remarkable feature of InGaN/GaN quantum well LEDs is that they emit intense light, reaching internal quantum efficiency of 95% [1] and external quantum efficiency of 85% [2]. The widely-believed solution to the above problem, in the 2000's, was that InGaN was an unstable alloy and that the indium in the InGaN quantum wells formed In-rich clusters, which were observed by Transmission Electron Microscopy (TEM) [3,4]. These low potential-energy regions were supposed to localize carriers and prevent them from reaching non-radiative centers such as dislocations, as observed by cathodo/photo luminescence [5, 6, 7, 8].

However, in the latter work [8], localization was observed without clear evidence of In cluster. Soon after, it was demonstrated that In rich clusters could be induced by the TEM observation itself [9], and more careful observations led to the conclusion that InGaN was a random alloy [10,11]. In recent years, Atom Probe Tomography (APT) has been used to tackle this issue on polar [10, 12] and non-polar [12, 13] materials. Studies agree that polar InGaN is a random alloy, while conclusions are not so clear for non-polar InGaN. Limitations of the observation technique have been described in terms of spatial resolution and quantitative issues [14]. In order to conclude that InGaN is a random alloy or not, the histogram of In content is compared with the one theoretically expected from a binomial distribution or its Gaussian limit. Unfortunately, this comparison often remains qualitative and lacks a measure that quantifies how far the measured distribution is from the theoretical one.

From the theoretical point of view, thermodynamics predicts spinodal decomposition [15]. However, additional effects have to be taken into account, which leads to more nuanced conclusion [16]. In particular, it is recognized that kinetic phenomena occurring on the surface during growth are of prime importance and may dominate the clustering/non clustering processes. In addition, composition pulling is also mentioned in InGaN/GaN heterostructures, in relation with experimental observations [17-22]. Finally, energy calculations in In rich cluster conclude that such clusters are rather unlikely but could exist and have an impact on optical properties [23].

Two main conclusions can be drawn from this overview. First, thermodynamics considerations predicting phase separation seem to be contradicted by experimental observations and it appears that kinetic processes occurring on the surface during growth should be considered. Second, a more quantitative estimation of the clustering degree should be introduced as simply opposing clustering and random alloy is not sufficient to describe the InGaN alloy. These are the two objectives of this work. To address them we use kinetic Monte Carlo simulations to describe the incorporation, desorption, and surface mobility of In and Ga atoms on the surface of InGaN during growth, and we address the In clustering and composition pulling effects, which correspond respectively to lateral and vertical inhomogeneities in InGaN thin films. The trends for In incorporation found in this paper, as well as the quantitative criterion for discussing clustering effects, should find their perfect playground in the heterostructures currently being developed to achieve red-emitting nitride LEDs, where In contents larger than 25% are systematically exploited. To achieve such large In contents, substrates with an in-plane lattice

parameter larger than that of GaN have been introduced. InGaN alloys with In contents between 25 and 30 % were obtained at UCSB on compliant porous GaN templates [24, 25] with InGaN layers underneath the quantum wells displaying just a few percents of In. Alternatively, Dussaigne *et al.* [26] obtained InGaN layers with up to 40% In by using InGaNOS pseudosubstrates, which include a relaxed InGaN layer with about 8% In. Finally, it is worth noting that the very large Wall Plug Efficiencies (WPEs) reported by Jiang and collaborators [27, 28] for yellow and red LEDs require the use of high-quality 30% and 40% In-content QWs in the active region (besides the exploitation of V-pits for efficient electrical injection), which are grown atop of a GaN/In_{0.1}Ga_{0.9}N superlattice, similar to Zhuang and collaborators [29]. Thus, the current work provides insight into the mechanisms operating in such large In-content alloys and defines a measure of In clustering whose interest will become apparent when analyzing quantitatively their statistical properties (e.g. by TEM and/or APT)".

2- Monte Carlo modeling

InGaN alloys consists in two element-III atoms (In and Ga) and one element-V atom (N). As it is usually done in this case [30-32], the modeling considers column III atoms only and assumes that N is not the limiting species or, more precisely, N is not playing any role in the relative processes (incorporation/desorption/surface mobility) of Ga and In atoms (relative means for instance that N does favor the incorporation of In compared to Ga). In addition, N is known to be less mobile on the surface than Ga or In [33].

Polar wurtzite nitrides are considered. The (0001) surface consists in two series of atomic sites separated by one monolayer (ML) (ABAB stacking). One defines the vertical columns along z containing group III atoms. The intersection between columns and monolayers define points, half of them being occupied by a group III atom. A full monolayer is thus defined here by an occupancy factor of 50%.

Three processes are taken into account and each of them is characterized by a rate per second. The first one is the deposition. The probability for an atom to be deposited is the same for all sites, and deposition rate on each atomic site is given by the nominal growth rate in monolayer per second. The Ga and In relative deposition rates depend on the stoichiometry of the incoming flux. We have modeled incoming stoichiometries of 10, 20 and 50 % In.

The second process is the desorption of an atom from the surface. Its rate depends on the barrier energy E_{des} associated with the process.

$$\Gamma_{des} = \Gamma_0 e^{-\frac{E_{des}}{kT}} \quad (1)$$

The prefactor Γ_0 accounts for the number of vibrational modes and is taken to be 10^{12} s^{-1} . The desorption energy is the atom surface energy. This value is given for an isolated atom on a flat surface and equals 1 eV for GaN [32] and 0.86 eV for InN. In this case, the atom has three nearest neighbors underneath (in this paper, the nearest neighbors (NN) mean column III atom nearest neighbors). If the surface is not flat or the atom is not isolated, then the NN number is smaller or larger than three and the energy must be modified accordingly: we use an energy of 0.3eV per additional Ga-Ga NN [32], 0.26 for In-In NN and 0.28 for In-Ga NN. Hence, an atom without NN would have a desorption energy of $1-3 \times 0.3 = 0.1 \text{ eV}$, very close to zero,

corresponding to a free atom, as it can be seen in plasma Molecular Beam epitaxy (MBE) with a Ga layer (or bilayer) on the surface under a Ga excess. Energies for In surface atoms have been estimated based on the bulk bond energies of InN and GaN [34].

The third process is the local reconfiguration of the surface. Atoms on the surface can break bonds and move to a neighboring site, leading after some repeats of this process, to surface diffusion. As the number of bonds to break is smaller than for desorption, the barrier energies are smaller. Various atomic movements can be identified at the atomic scale, each of them associated with a given energy [35]. We restricted our choice to the most likely event, corresponding to the smallest energy, 0.79 eV for GaN. We extrapolated an energy of 0.68 eV for the corresponding process in InN, based on the atomic surface energies discussed above. These energies are corrected, as for the desorption, to account for the exact number of NN. For each atom jump, the authorized destination sites are identified: atoms can only jump to sites at the same level as or below the initial site, as moving to a higher level would require breaking more bonds. The arrival site is randomly chosen with the same probability among all authorized sites. A more refined description of the surface with the nature of the steps exists [36] which allows to discuss the Ehrlich-Schwöbel barrier and how the surface morphology evolves. These details (e.g. the coexistence of A- and B-type step edges with different dangling-bond configurations) are not necessary for our purpose and, moreover, the related parameters to be used would become largely arbitrary in the case of alloys, so we chose a simplified version of the atom jumps with less free parameters.

The last and fundamental ingredient that we need to introduce is the local elastic energy. Indeed, In is a bigger atom than Ga and bonds are distorted both in the volume and at the surface. Surface reconstruction also occurs in order to minimize the related elastic energy [37, 38]. The effect of strain on the formation enthalpy of an isolated Ga or Al atom on a surface as a function of strain has been estimated, showing that the strain modifies this energy by about 0.4 eV [39]. Lymperakis and coworkers [40] have calculated by Density Functional Theory (DFT) the energies of the associated reconstructed surface for a 1 ML of InN grown on GaN. While In can be incorporated with no energy penalty in $\frac{1}{4}$ of the sites, adding more In costs about 0.3eV per In atom, which tends to limit the In content to 25% in InGaN layers coherently grown on GaN. However, elastic energy calculated by DFT is not available in all configurations for the InGaN alloys and we must rely on simpler approaches and approximations. We have used the classical elastic energy calculation for a thin film epitaxially grown on a lattice mismatch substrate, and the corresponding in plane strain ϵ_{xx} :

$$W=(c_{11} + c_{12} - 2 \frac{c_{13}^2}{c_{33}})\epsilon_{xx}^2 \quad (2)$$

where the elastic constants are the usual ones [41, 42].

We can derive the energy per atom by dividing this energy per unit volume by the number of atoms in the unit cell and multiplying by its volume. One finds energies of 1.15eV for InN on GaN and 1.52 eV for GaN on InN. For alloys, the energy scales with the square of the strain i.e. the square of the alloy composition. We neglect here any plastic relaxation. The above derivation holds for an entirely filled 2D film. During the growth, terraces and steps form on the surface and allow for elastic relaxation minimizing thereby the total elastic energy. We take this relaxation into account for each atom by considering the number NNN of nearest neighbors. If the atom is inside a continuous film, it has 6 NN in the plane and 3 NN below it, and there is

no relaxation. On the contrary, an adatom without NN below and around it (NNN=0) is fully relaxed, and the elastic energy is zero. In intermediate cases, we simply interpolate and the elastic energy calculated in (2) is multiplied by NNN/9. At the end, we find an elastic energy which is on the order of 0.4-0.5 eV for an isolated atom on a surface, similar to the value calculated by DFT for the case of AlN and GaN [39].

At this stage, it is important to comment the approximations that we made to estimate the energies. We cannot access the exact values, which, anyway, depend on the environment (gases and molecules) above the surface, and cannot be unique. Quantum calculations face the same problem. These energies will be used to calculate process rates, with an exponential temperature activation. An error in the energy will simply shift the temperature at which the process is activated. Hence, we must be aware that the temperatures that will be given later in this paper as the onset of a given process are indicative only. This, however, will not alter the general conclusions.

For obvious reasons of computation time, the modeled area is limited to $30 \times 60 = 1800$ atomic sites along x and y , and 10 atomic sites in the vertical direction z for each column (20 monolayers). This corresponds to horizontal dimensions L_x and L_y of $45a$ (14nm) and $30\sqrt{3}a$ (16 nm) respectively (with the in-plane parameter $a=0.31$ nm), which is the typical size of APT maps [13]. In order to mimic an infinite surface and avoid accumulation or desertion at the boundaries, we use periodic conditions both along x and y . When the initial surface is flat, we use strict periodic conditions:

$$f(x + L_x, y + L_y, z) = f(x, y, z) \quad (3)$$

where $f(x, y, z)$ describes the occupation of the atomic site of position x, y, z . When we use an off-axis surface, with steps and terraces, and a difference of height equal to h along a distance of, say, L_x , we impose quasi-periodic conditions:

$$f(x + L_x, y + L_y, z + h) = f(x, y, z) \quad (4)$$

This condition imposes that the general offcut angle of the surface is kept constant during the growth, which corresponds to the experimental observation. We have limited the study to off-axis surfaces to two mono-atomic steps ($h=0.5$ nm) in the surface along the distance of 14 nm, which corresponds to a misorientation angle of 2° . Note that two steps are inserted in order to observe eventual step bunching. Such a misorientation is larger than the one usually used for growing InGaN on GaN-on-sapphire templates, which is about 0.2° . A 0.2° misoriented surface would require a large area (70 nm wide) in order to include one atomic step, and even larger (140 nm) to include two steps. Such a large area would induce long computation times and cannot be reasonably modeled. Note that, as will be shown later, step flow will occur at high temperature. In this case a smaller miscut angle, and correspondingly wider terraces, would merely lead to a step flow mode occurring at a slightly higher temperature.

Once the layer is grown, the occupation function f is known for all atomic sites (about 18000 atoms) and we can calculate all macroscopic parameters such as the mean In content, the surface morphology, the surface profile along any direction (in particular along step direction), and the In content integrated along individual vertical columns. In order to compare with APT maps that display a nanometer spatial resolution, we also provide the In content integrated along 10 neighboring columns (i.e. one reference column, 3 nearest columns at a distance of a , 6 second

nearest columns at a distance of $\sqrt{3}a$). Each calculation was performed between 4 and 7 times and macroscopic parameters are averaged over these runs.

The calculation was performed for temperatures ranging from 300°C to 1000°C (or less in some cases). At low temperature, atom evaporation and diffusion are limited, and the most likely events are the deposition events. The calculation of the growth is fast, it takes a few minutes on a PowerEdge R930 [43]. At high temperature, however, atom diffusion dominates and atom jumps are the most likely event. The calculated growth is slow and the computation time increases up to tens of hours.

The initial layer, which cannot be modified (no evaporation nor jump), contains two GaN monolayers, so that each column contains one initial Ga atom. For off-axis surfaces, one or two non-removable monolayers are added in order to build steps and terraces.

3-Results and discussion

We first discuss the surface morphology. Fig.1 shows the occupancy of the layers as a function of their vertical position. The target growth is 20 monolayers so that the total target thickness is 22 monolayers. If the layer would be perfectly smooth, all monolayers up to the 22nd would be full (50% occupancy) and all layers above would be empty (0% occupancy). At low temperature, some layers below the 22nd layer are not full and some layers above are partially occupied, representing surface roughness. As the growth temperature increases, the transition between fully occupied and empty layers becomes more and more abrupt: the surface becomes atomically smooth. This is the regime of layer-by-layer growth, which can be followed by Reflection High Energy Electron Diffraction (RHEED) oscillations in MBE. It occurs at sufficiently high temperature when the atom mobility on the surface is high enough: islands nucleate on atomic terraces and then grow until a full layer is completed, recovering an atomically smooth surface.

On off-axis surfaces (see Fig. 2), the same process can be observed except that steps are maintained by the quasiperiodic conditions. Atoms move from terraces to steps, which move forward at high temperature: this is the step flow growth regime where the steps remain clearly visible in the profile. At low temperature, nucleation occurs on the terraces so that steps do not remain aligned along their initial direction and disappear from the profile. This surface morphology was obtained for all In compositions. The evolution of roughness with temperature is an important parameter for the evaluation of the In composition and its lateral fluctuations. Indeed, lateral thickness fluctuation of a few units are non-negligible compared to the total thickness of 20 monolayers. When calculating the In content per column (number of In atoms divided by total number of atoms), such thickness fluctuations will lead to In content fluctuations. Hence, the layer roughness at low temperature will lead to spatial fluctuations of the composition. These fluctuations of thickness have an impact on the composition integrated along z for thin layers. This effect can be particularly important for quantum wells, where the electron and hole energies will be impacted, possibly creating lateral carrier localization.

Next, we study the mean indium content in the layer. As observed experimentally, the computed indium content decreases as the growth temperature increases. Figure 3 shows that this decrease is the same for on-axis and for off-axis orientations. The observed variation of indium content as a function of growth temperature [44,45] is actually much stronger than the one calculated here, which indicates that the difference in bonding energies between Ga and In is larger than

the one we have used. The second difference between our result and the experimental one is the In-incorporation dependence on misorientation. We observe the same In content in InGaN layers grown on perfectly oriented surfaces and on 2° off surfaces. While this is not always observed, the indium content is reported to vary with misorientation in some publications on Ga-polar faces [45, 46] and N-polar faces [47]. The explanation for the Ga-polar face is the following: as steps flow faster, the incoming Ga atoms prevent the evaporation of In from the terraces more efficiently thereby increasing the mean In content. Hence, the In content was observed to decrease with miscut angle from 13% for 0.2° to 8% for 1.8° [46]. This effect operates only when In and Ga have very different sticking coefficients and in the step flow growth mode, and for instance does not operate in InAlN where the growth is 3D [46]. For the N-polar face, multi-atomic steps tend to develop and growth on new facets reduces the In incorporation [47]. First, our model is related to Ga face surface and we exclude considering new facets and incorporation on new facets. Second, our results suggest, as already said, that we underestimated the difference in bonding energies between In and Ga, meaning that the difference in sticking coefficients between In and Ga may be underestimated. Third, we did not investigate various off cut angles, so that we cannot directly compare with experimental results [45,46]. Fourth, when treating the perfectly oriented surface, we observe that islands nucleate on terraces (easily at low temperature, while with difficulty and more slowly at high temperature) and then grow until the surface becomes flat and then the process repeats. This is intrinsically due to the periodic boundary conditions and the small area which can be modeled. During the island growth, In incorporates on the island edges as it incorporates on step edges on miscut surfaces. Hence, it may explain why our model gives the same In content for 0 and 2° off cuts. To conclude, it seems that our model cannot reproduce the variation of step flow speed and the related variation of In incorporation with miscut angle.

We now study the In content profile in the layer. In order to magnify the effect, we will focus on layers grown with an incident In content of 50%. Figure 4 shows the In profile for various growth temperatures. The In content increases as the growth proceeds and finally saturates to its equilibrium value, which decreases with increasing temperature (as shown in Fig. 3). The In content values in Fig.4 are actually normalized by this equilibrium value so that all profiles tend to unity. This allows to better see the In content transient along the growth direction, the amplitude and spatial extension of which increases with increasing temperature. This is the well-known composition pulling effect: when growing InGaN on GaN, the strain reduces the In incorporation. As the lattice parameter at the surface varies with In content, the In incorporation becomes easier, and the In content reaches its equilibrium value. In order to evidence that this pulling effect is due to strain, we have calculated in Fig.5 the same profiles with an elastic energy twice larger than the one used in Fig.4. We observe that the composition transients are much larger both in amplitude and in spatial extension when the elastic energy is larger. Similar results are obtained with off-axis orientations. Composition pulling is due to strain and is permitted when the temperature is high enough to allow for sufficient atom mobility on the surface. Note that, incidentally, in Figure 5 the In content in the first InGaN layer (deposited on GaN) has an indium content of 50% of the impinging nominal value, which in the present case equals 50%; this leads to an In content in the first monolayer of 25%, which corresponds to the maximum In mole fraction calculated by Lymperakis *et al.* [40] for a coherently-grown InGaN layer on pure GaN. However this result is obtained for an elastic energy twice the value calculated from the macroscopic elastic theory.

We finally turn to the lateral In fluctuations, which are the core of this study. First, we show in Fig.6 the maps of In content in two layers grown at two different temperatures, with the same indium content equal to 19% (the incident In flux is 19% at low temperature and has been adjusted at high temperature to reach the same equilibrium content in the layer). The content is laterally averaged over 10 columns. The growth was limited here to 10 monolayers and the strain energy was doubled to magnify the effect. One observes lateral fluctuations of composition, which are much frequent at higher temperature. This gives us a first evidence that more In fluctuations appear at higher temperature. In order to be more quantitative, we introduce now a parameter that we call cluster index. In a statistical InGaN alloy, composition fluctuations are due to the random distribution of In and Ga atoms. Within n atoms, the probability to get k In atoms is given by the binomial law:

$$p(k) = \frac{n!}{k!(n-k)!} p^k (1-p)^{n-k} \quad (5)$$

where p is the average probability to get an indium atom, equal to mean In content.

The average Indium content is p and its standard deviation is $\sqrt{\frac{p(1-p)}{n}}$.

For sufficiently large numbers, this binomial law tends to a Gaussian law. The probability to get an indium content equal to x is given by:

$$p(x) = \frac{1}{\sqrt{2\pi}\sigma} e^{-\frac{(x-x_{mean})^2}{2\sigma^2}} \quad (6)$$

with $x_{mean}=p$ and $\sigma = \sqrt{\frac{p(1-p)}{n}}$. Note that, for instance, for 20 monolayers and 10 columns we get n=100. For an average In content of 25%, we get a Gaussian distribution centered at x=0.25 with a width $\sigma=0.043$. We will compare the calculated distribution with the Gaussian one and calculate the cluster index C which is the deviation to the Gaussian law:

$$C = \sum_m abs(histo(m) - p(x_m) \times \Delta) \quad (7)$$

We typically use histograms with m=50 intervals of value Δ , and we normalize the histograms by the number of points (1800). C is thus analogous to a probability. The statistical alloy is characterized by C=0, and C reaches a fraction of unity for large deviations from the statistical alloy. Introducing this quantitative and continuously varying parameter allows to go beyond the usual binary discussion about the presence or not of fluctuations. We verified that at low temperature, the distribution is close to a Gaussian one and C is small. C is however not equal to zero because of the thickness fluctuations mentioned above. Figure 7 shows the cluster index for layers grown on-axis and off-axis at various temperatures and with an incident In content of 25%. We observe that C is constant and small at low temperature, reaches a minimum around 700-800°C and then increases at high temperature. The behavior is similar for both on- and off-axis orientations. At the sweet spot around 700-800°C, the temperature is high enough to provide smooth surfaces and low enough to lessen In surface diffusion and its associated clustering. Similar results are obtained with 10% incident In.

In order to evidence the origin of the clustering at high temperature, we focus on layers grown with 50% incident In, and we will vary the amplitude of the elastic energy. Figure 8 shows the cluster index for InGaN layer grown off-axis with 50% incident In calculated either per atomic column or averaged over 10 atomic columns. The calculation is performed either taking into account the elastic energy (doubled) or setting it to zero. We observe that the cluster index increases with temperature when the elastic energy is taken into account, while it remains constant and weak if the strain is not taken into account. Again, a sweet spot appears as a trade-off between roughness and clustering, at 500°C, at a lower temperature than for In poor layers. A similar behavior is observed on-axis (Fig.9) with the same sweet spot at 500°C, but with a smaller cluster index. While In incorporation on steps in off-axis surfaces could be expected to be faster and to reduce the clustering, the contrary is observed. Interestingly, the same observation was made experimentally [48]. Finally, we show in Fig.10 the cluster index for InGaN grown on-axis with 50% incident In as a function of temperature and for various elastic energies. We clearly observe that the clustering at high temperature is due to the elastic energy. As energies appear in an exponential term, it was expected that clustering and its index do not vary linearly with the energies.

Results show that two phenomena appear at high temperature and are due to the strain: the composition pulling effect and the clustering. Both simply express that atomic jumps are thermally activated, and preferred incorporation sites are those which minimize the elastic energy. Along the growth direction, In atoms tend to segregate and incorporate further when the In composition is higher and the mean lattice parameter is larger. Laterally, In atoms diffuse on the surface and tend to incorporate themselves into In-rich regions where the lattice parameter is larger and the elastic energy is smaller. Once an In-rich cluster is created, In atoms tend to incorporate on its surface. However, atom incorporation remains only partially deterministic, and an In-rich cluster may be fully recovered by Ga atoms, leading to 3D In-rich clusters. Hence, clustering is not restricted to the 2D growth plane but can (and does) also happen along the growth direction. All these processes occur dynamically on the surface. Hence, composition pulling and clustering are both consequences of the same surface physics: Strain is the cause of these processes, and temperature is the parameter allowing them to happen. Growing at higher rate will shift the occurrence of these processes to higher temperature, but the shift will remain limited as the temperature has an exponential impact while the growth rate has a linear effect. As already explained, the amplitude of the aforementioned processes and the temperature at which they appear may not be exact, as the involved energies are not precisely known. In particular, we recognize that the temperature dependence of the In incorporation is larger than the one found in our paper (Fig. 3). However, the general trend remains. Let us also recall that we did not take into account structural defects, in particular dislocations, which may alter the conclusions. Additional phenomena, such as step meandering, which are not taken into account in our model where isotropic atomic jumps only are considered, may also have an impact on disorder, as experimentally shown [49]. Based on our simplified and isotropic model for atomic jumps, we cannot describe the surface instabilities that have been observed in various materials (Ehrlich-Schwoebel, Grinfeld, Bales-Zangwill, Wolf–Villain, ...) as described in [50] for instance. These phenomena are of prime importance for the surface morphology, but can be expected to be of second order for the In content fluctuations if In and Ga behave the same in regards of these instabilities. In addition, some of these instabilities lead to very rough surfaces and are unlikely to happen in the high quality InGaN layers used to fabricate LEDs and lasers, which are those used to study In clusters.

Furthermore, for high indium contents, a 2D-3D Stranski-Krastanov transition may occur when the elastic energy contained in the whole layer exceeds a given value. This transition cannot be taken into account in our model as we consider only the elastic energy contained in the last monolayer. Our results remain thus valid for thin layers which remain 2D.

Currently, it is believed/claimed that InGaN layers grown for high performances devices do not exhibit In rich clusters beyond the statistical limit. We believed that it simply means that they are grown within the sweet spot mentioned in this paper. Growing at higher temperature would create clusters, as demonstrated by annealing InGaN layers grown at lower temperature, although processes occurring in the bulk differ from surface kinetics. However, the comparison with experimental results should be done carefully, as growing at higher temperatures leads experimentally to a reduced In content (more severely than in our model, as already noticed when commenting Fig.3). In order to keep a large enough In content in the films while growing at high temperature, the In flux should need to be considerably increased, leading to possible In droplet formation and a strongly degraded quality, which will probably preclude such a theory-experiment quantitative comparison.

The objective of this paper was to explain the absence of clear separation between statistical alloys and alloys with clusters, and the clustering index describes this continuous transition. Experimentally, the spatial and absolute resolution provided by APT and TEM is already high enough to assess this clustering index, which is thus a relevant and meaningful parameter that could be used to benchmark results of different groups.

4. Conclusion

We modeled the growth of InGaN alloys on perfectly oriented and misoriented GaN surfaces. As the growth temperature increases two distinct phenomena occur: composition pulling and In-rich cluster formation. Both are caused by the strain due to the lattice mismatch between GaN and InGaN and the related elastic energy. Indium lateral diffusion and vertical segregation are thus two facets of the same surface physics, both related to strain, and lead to cluster formation and composition pulling respectively. The transition between statistical alloys described by a binomial distribution law and heterogeneous layers with In-rich clusters has been shown to be smooth as a function of growth temperature; to quantify the degree of clustering within the InGaN layers we have introduced a cluster index, which is shown to increase above a given temperature and which we propose as a means to compare quantitatively results by different groups. Below this temperature, surface roughness leads to apparent composition fluctuations, which could be of importance in quantum wells. Above this temperature, In-rich clusters progressively form. This temperature thus defines the optimum InGaN growth temperature, which decreases with the indium content.

References

- [1] C. A. Hurni, A. David, M. J. Cich, R. I. Aldaz, B. Ellis, K. Huang, A. Tyagi, R. A. DeLille, M. D. Craven, F. M. Steranka, M. R. Krames, *Appl. Phys. Lett.* **106**, (2015), 031101. <https://doi.org/10.1063/1.4905873>
- [2] Y. Narukawa, M. Ichikawa, D. Sanga, M. Sano, T. Mukai, *J. Phys. D: Appl. Phys.* **43**, (2010) 354002. <http://dx.doi.org/10.1088/0022-3727/43/35/354002>
- [3] S. Chichibu, T. Azuhata, T. Sota, S. Nakamura, *Appl. Phys. Lett.* **69**, (1996) 4188
- [4] Y. Narukawa, Y. Kawakami, M. Funato, S. Fujita, S. Nakamura, *App. Phys. Lett.* **70**, (1997) 981
- [5] S. Chichibu, K. Wada, S. Nakamura, *Appl. Phys. Lett.* **71**, (1997) 2346. <doi.org/10.1063/1.120025>
- [6] K. P. O'Donnell, R. W. Martin, P. G. Middleton, *Phys. Rev. Lett.* **82**, (1999) 237.
- [7] H. Schömig, S. Halm, A. Forchel, G. Bacher, J. Off, F. Scholz, *Phys. Rev. Lett.* **92**, (2004) 106802. <doi.org/10.1103/PhysRevLett.92.106802>
- [8] D. M. Graham, A. Soltani-Vala, P. Dawson, M. J. Godfrey, J. S. Barnard, M. J. Kappers, C. J. Humphreys, *Journal of Applied Physics* **97**, (2005) 103508. <https://doi.org/10.1063/1.1897070>
- [9] C. J. Humphreys, *Philosophical Magazine* **87**, no. 13, (2007) 1971. <doi:10.1080/14786430701342172>.
- [10] M. J. Galtrey, R. A. Oliver, M. J. Kappers, C. J. Humphreys, P. H. Clifton, D. Larson, D. W. Saxey, A. Cerezo, *J. of Appl. Phys.* **104**, (2008) 013524.
- [11] T. Schulz, T. Remmele, T. Markurt, M. Korytov, M. Albrecht, *Journal of Applied Physics* **112**, (2012) 033106. <doi.org/10.1063/1.4742015>
- [12] C.J. Humphreys, J.T. Griffiths, F. Tang, F. Oehler, S.D. Findlay, C. Zheng, J. Etheridge, T.L. Martin, P.A.J. Bagot, M.P. Moody, D. Sutherland, P. Dawson, S. Schulz, S. Zhang, W.Y. Fu, T. Zhu, M.J. Kappers, R.A. Oliver, *Ultramicroscopy*, **176**, (2017) 93. <doi.org/10.1016/j.ultramic.2017.01.019>
- [13] H. Li, M. Khoury, B. Bonef, A. I. Alhassan, A. J. Mughal, E. A., Muhammad E.A. Samsudin, P. De Mierry, S. Nakamura, J. S. Speck, S. P. DenBaars, *ACS Appl. Mater. Interfaces* **9**, 41, (2017) 36417. DOI: 10.1021/acsami.7b11718;
- [14] L. Rigutti, B. Bonef, J. Speck, F. Tang, R. A. Oliver, *Scripta Materialia*, **148**, (2018) 75. <doi.org/10.1016/j.scriptamat.2016.12.034>
- [15] I-H. Ho and G. B. Stringfellow, *Appl. Phys. Lett.* **69**, (1996) 2701. <https://doi.org/10.1063/1.117683>

- [16] G.B. Stringfellow, *J. Cryst. Growth* 312, (2010) 735 . doi:10.1016/j.jcrysgro.2009.12.018
- [17] Y. Kawaguchi, M. Shimizu, M. Yamaguchi, K. Hiramatsu, N. Sawaki, W. Taki, H. Tsuda, N. Kuwano, K. Oki, T. Zheleva, R. F Davis, *J. Cryst. Growth* 24, (1998) 189 .
- [18] S. Pereira, M. R. Correia and E. Pereira, K. P. O'Donnell, C. Trager-Cowan, and F. Sweeney E. Alves, *Phys. Rev. B.* 64, (2001) 205311.
- [19] M.R. Correia, S. Pereira, E. Pereira, J. Frandon, I. M. Watson, C. Liu, E. Alves, A. D. Sequeira, N. Franco, *Appl. Phys. Lett.* 85 (2004) 2235.
- [20] H.Y. Lin, Y.F. Chen, T.Y. Lin, C.F. Shih, K.S. Liu, N.C. Chen, *J. Cryst. Growth* 290 (2006) 225.
- [21] C.B. Soh, S.J. Chua, P. Chen, D.Z. Chi, W. Liu, H. Hartono, *Thin Solid Films* 515 (2007) 4509.
- [22] M. Pristovsek, J. Stellmach, M. Leyer, M. Kneissl, *Phys. Status Solidi C* 6 (2009) 5565.
- [23] L. C. de Carvalho, A. Schleife, J. Furthmüller, F. Bechstedt, *Phys. Rev. B* 85, (2012) 115121.
- [24] S. S. Pasayat, C. Gupta, M. S. Wong, R. Ley, M. J. Gordon, S. P. DenBaars, S. Nakamura, S. Keller, and U. K. Mishra, *Applied Physics Express* 14, 011004 (2021).
- [25] P. Chan, S. P. DenBaars, and S. Nakamura, *Appl. Phys. Lett.* 119, 131106 (2021).
- [26] A. Dussaigne, F. Barbier, Damilano, S. Chenot, A. Grenier, A. M. Papon, B. Samuel, B. Ben Bakir, D. Vaufrey, J. C. Pillet, A. Gasse, O. Ledoux, M. Rozhavskaaya, and D. Sotta, *J. Appl. Phys.* 128, 135704 (2020).
- [27] F. Jiang, J. Zhang, L. Xu, J. Ding, G. Wang, X. Wu, X. Wang, C. Mo, Z. Quan, X. Guo, C. Zheng, S. Pan, and J. Liu, *Photonics Research* 7, 2 , 144 (2019) .
- [28] S. Zhang, J. Zhang, J. Gao, X. Wang, C. Zheng, M. Zhang, X. Wu, L. Xu, J. Ding, Z. Quan, and F. Jiang, *Photonics Research* 8, 1671, (2020).
- [29] Z. Zhuang , D. Iida, and K. Ohkawa , *Jpn. J. Appl. Phys.* 61 SA0809 (2022).
- [30] N. Grandjean and J. Massies, *J. of Crystal Growth* 134, (1993) 51.
- [31] N. Grandjean, J. Massies, M. Leroux, *Phys. Rev. B* 53, (1996) 998.
- [32] N. A.K. Kaufmann, L. Lahourcade, B. Hourahine, D. Martin, N. Grandjean, *J. of Crystal Growth* 433, (2016) 36.
- [33] T. Zywietz, J. Neugebauer, M. Scheffler, *Appl. Phys. Lett.* 73, (1998) 487. doi.org/10.1063/1.121909
- [34] *Handbook of Nitride Semiconductors and Devices. Vol. 1.* Hadis Morkoç, Copyright ©2008 WILEY-VCH Verlag GmbH & Co. KGaA, Weinheim, ISBN: 978-3-527-40837-5

- [35] M. Chugh and M. Ranganathan, *Applied Surface Science* 422, (2017) 1120. doi.org/10.1016/j.apsusc.2017.06.067. *Phys. Status Solidi C* 12, 4–5, 408 (2015). DOI 10.1002/pssc.201400194
- [36] T. Akiyama, T. Ohka, K. Nakamura, and T. Ito, *Journal of Crystal Growth*, 532, (2020) 125410. doi.org/10.1016/j.jcrysgro.2019.125410
- [37] A. L. Rosa and J. Neugebauer, *Phys. Rev. B* 73, (2006) 205346. doi.org/10.1103/PhysRevB.73.205346
- [38] M. Chugh and M. Ranganathan, *Phys. Chem. Chem. Phys.*, 19, (2017) 2111. DOI: 10.1039/c6cp07254b.
- [39] S. Lu, Z. Luo, J. Li, W. Lin, H. Chen, D. Liu, D. Cai, K. Huang, N. Gao, Y. Zhou, S. Li, J. Kang. *Nanoscale Res Lett* 17, (2022) 13. <https://doi.org/10.1186/s11671-022-03652-0>
- [40] L. Lymperakis, T. Schulz, C. Freysoldt, M. Anikeeva, Z. Chen, X. Zheng, B. Shen, C. Chèze, M. Siekacz, X. Q. Wang, M. Albrecht, and J. Neugebauer, *Physical Review Materials* 2, 011601(R) (2018).
- [41] K. Adachi, H. Ogi, A. Nagakubo, N. Nakamura, M. Hirao, M. Imade, M. Yoshimura, Y. Mori, *J. of Appl. Phys.* 109, (2016) 245111. doi.org/10.1063/1.4955046.
- [42] I. Vurgaftman and J. R. Meyer, *Journal of Applied Physics* 94, (2003) 3675. doi.org/10.1063/1.1600519.
- [43] Dell PowerEdge R930, 4 processors Intel Xeon E7-4850 v3 (2,2GHz, 14Cores/28Threads), memory 8×32Go LRDIMM. Software written in Matlab uses 56 cores.
- [44] W. Van der Stricht, I. Moerman, P. Demeester, L. Considine, E. Thrush, J. Crawley. *MRS Internet Journal of Nitride Semiconductor Research*, 2, E16 (1997). doi:10.1557/S1092578300001423
- [45] M. Sarzynski, M. Leszczynski, M. Krysko, J. Z. Domagała, R. Czernecki, T. Suski, *Cryst. Res. Technol.* 47, No. 3, (2012) 321 / DOI 10.1002/crat.201100491
- [46] M. Leszczynski, R. Czernecki, S. Krukowski, M. Krysko, G. Targowski, P. Prystawko, J. Plesiewicz, P. Perlin, T. Suski, *J. Cryst. Growth* 318, (2011) 469. doi.org/10.1016/j.jcrysgro.2010.10.050
- [47] Keller, S., Suh, C. S., Fichtenbaum, N. A., Furukawa, M., Chu, R., Chen, Z., Vijayraghavan, K., Rajan, S., Denbaars, S. P., Speck, J. S., & Mishra, U. K. (2008). *Journal of Applied Physics*, 104, (2008) 093510. doi.org/10.1063/1.3006132
- [48] G. Franssen, T. Suski, M. Kryško, B. Łucznik, I. Grzegory, S. Krukowski, A. Khachapuridze, R. Czernecki, S. Grzanka, P. Mensz, M. Leszczyński, S. Porowski, M. Albrecht, *Phys. Stat. sol. C*, 5, (2008) 1485. <https://doi.org/10.1002/pssc.200778409>
- [49] R. Butté, L. Lahourcade, T. K. Uždavinyš, G. Callsen, M. Mensi, M. Glauser, G. Rossbach, D. Martin, J.-F. Carlin, S. Marcinkevičius, N. Grandjean, *Appl. Phys. Lett.* 112, (2018) 032106; doi.org/10.1063/1.5010879

[50] A. Pimpinelli, J. Villain, *Physics of Crystal Growth* (Collection Alea-Saclay: Monographs and Texts in Statistical Physics), 1998 by Cambridge University Press, ISBN10: 0521558557

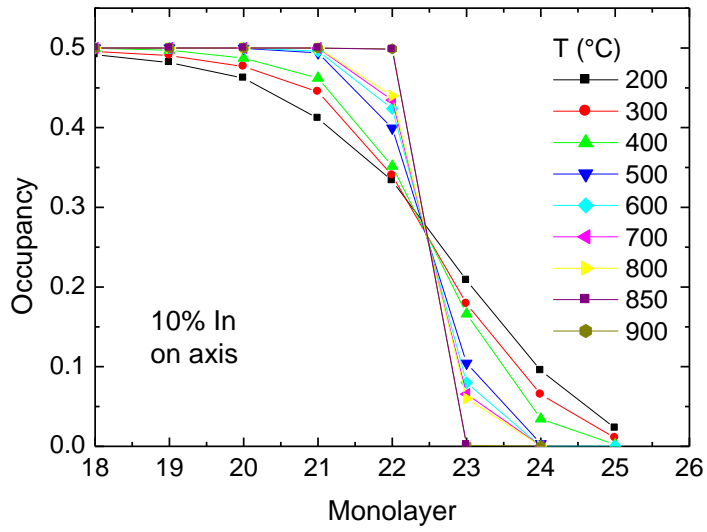


Figure 1: Occupancy factor of the monolayers as a function of their position along the growth direction in $\text{In}_{0.1}\text{Ga}_{0.9}\text{N}$ grown at various temperatures. The nominal thickness grown corresponds to 20 monolayers on top of a two monolayers template. The surface is on-axis.

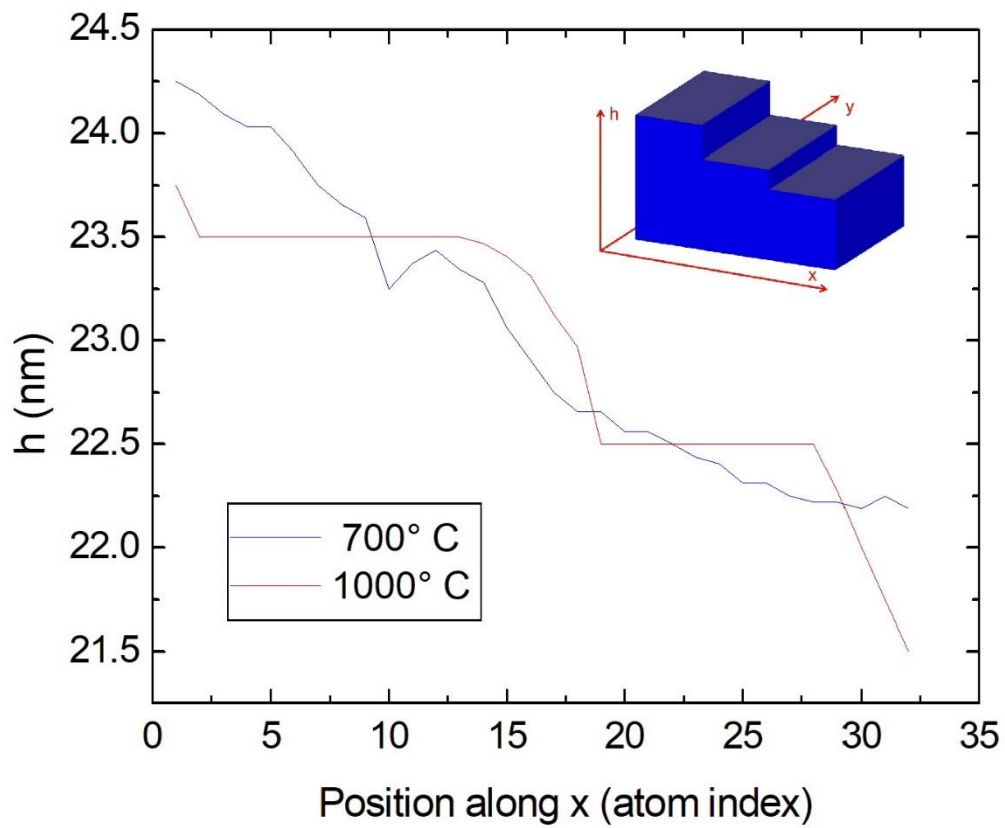


Figure 2: Profile of the $\text{In}_{0.1}\text{Ga}_{0.9}\text{N}$ layer observed along the y axis (parallel to the initial step direction, see inset), grown at two temperatures (700°C and 1000°C).

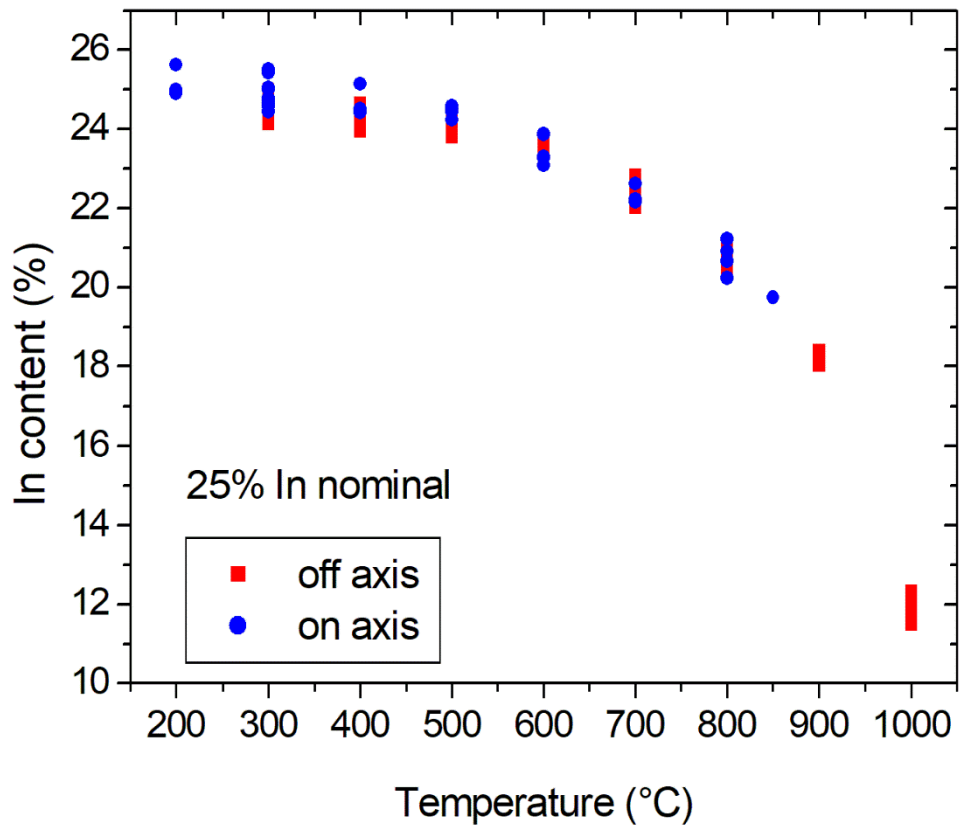


Figure 3 : Indium content averaged over the whole layer as a function of growth temperature for on-axis and off-axis orientations. The incident In content is 25%.

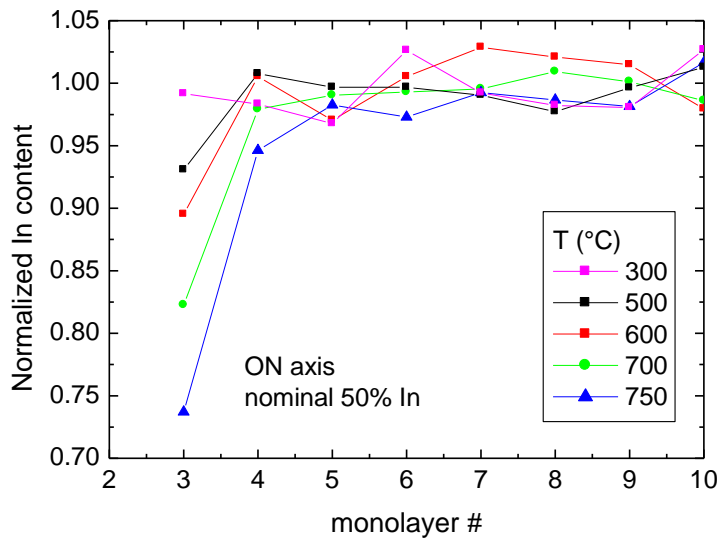


Figure 4 : Normalized In content profile in InGaN grown at various temperatures. The incident In content is 50%. The surface is on-axis. The In content is normalized by the In content in the last monolayers (50%, 48.5%, 46%, 44% and 42.6% at 300, 500, 600, 700 and 750°C respectively).

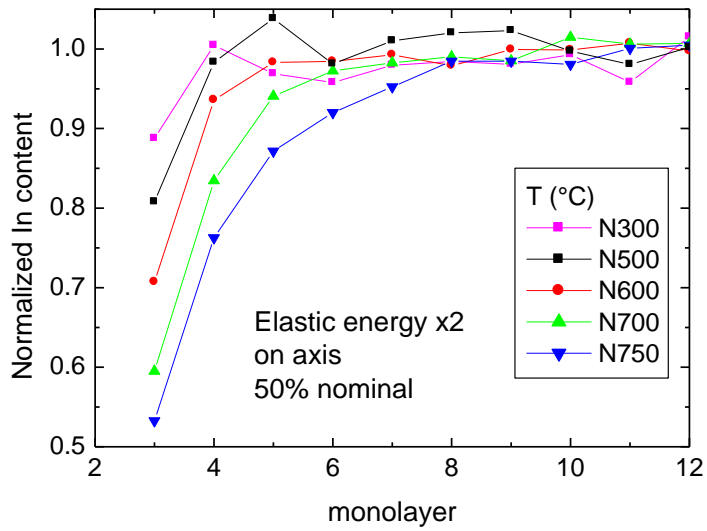


Figure 5 : Normalized In content profile in InGaN grown at various temperatures. The incident In content is 50%. The surface is on-axis. The In content is normalized by the In content in the last monolayers (50%, 47.5%, 46%, 42.7% and 41.4% at 300, 500, 600, 700 and 750°C respectively). Compared to Figure 4, the elastic energy due to strain is multiplied by 2.

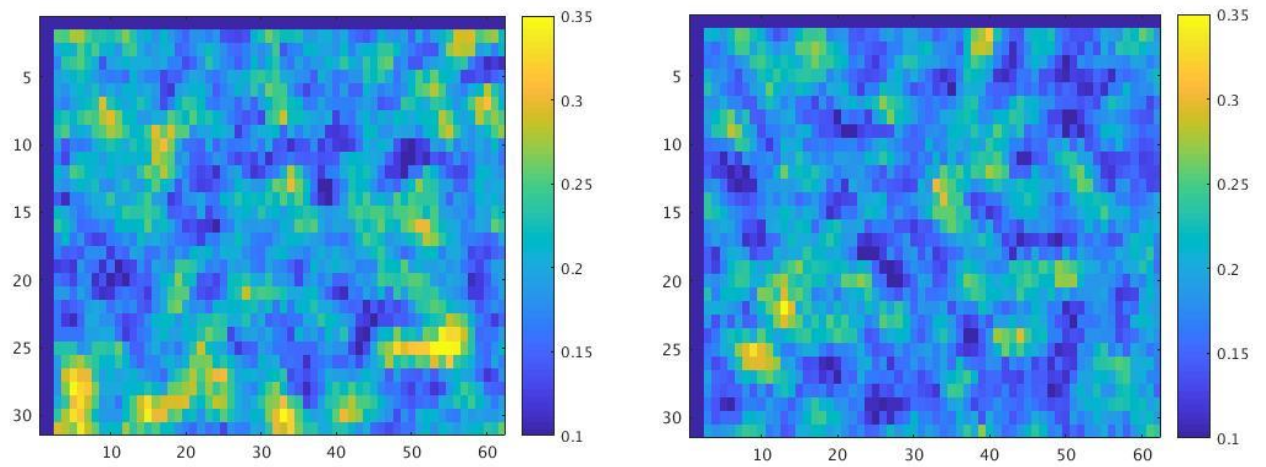


Figure 6: Maps of indium content (averaged laterally over 10 atomic columns) for InGaN layers grown at 300°C (right) and 700°C (left). The incident In flux is adjusted so that the final In content is the same in both layers (19%). On axis. Strain energy doubled. Thickness :10 monolayers

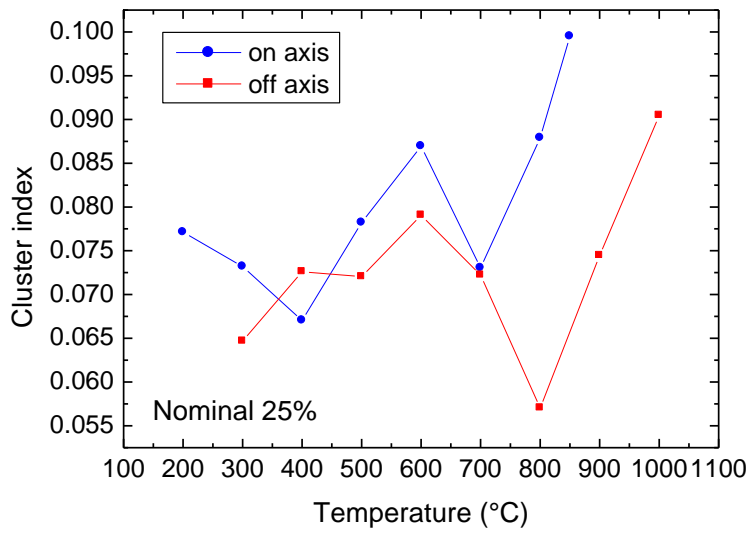


Figure 7: Cluster index for InGaN layers as a function of growth temperature for on-axis and off-axis orientations. The incident In content is 25%. The In content was averaged over 10 columns.

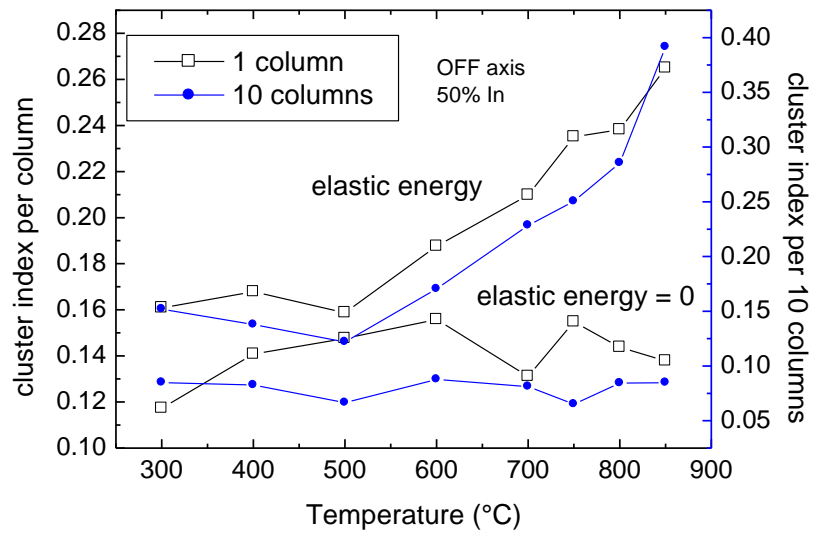


Figure 8: Cluster index for layers grown on off-axis substrate with 50% incident In, as a function of growth temperature. The index is calculated per atomic column or averaged laterally over 10 atomic columns. The energy related to the strain is set to double its value or set to zero.

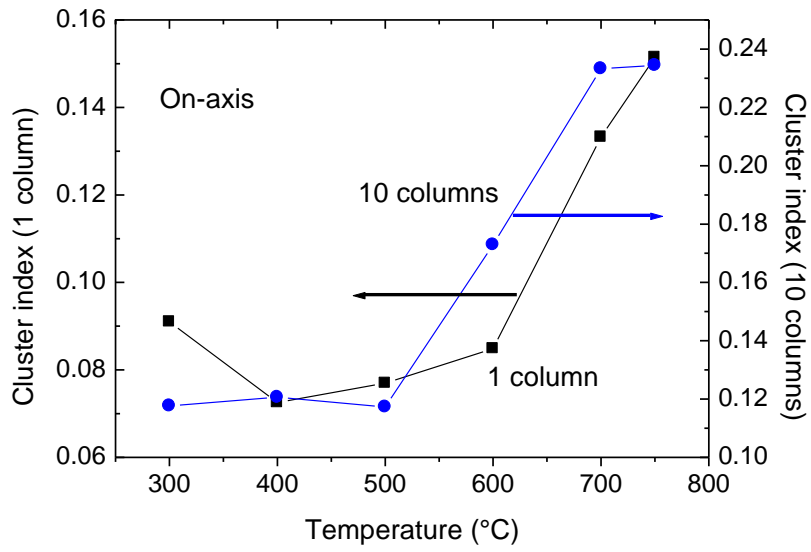


Figure 9: Cluster index for layers grown on on-axis substrate with 50% incident In, as a function of growth temperature. The index is calculated per atomic column or averaged laterally over 10 atomic columns. The energy related to the strain is set to double its value.

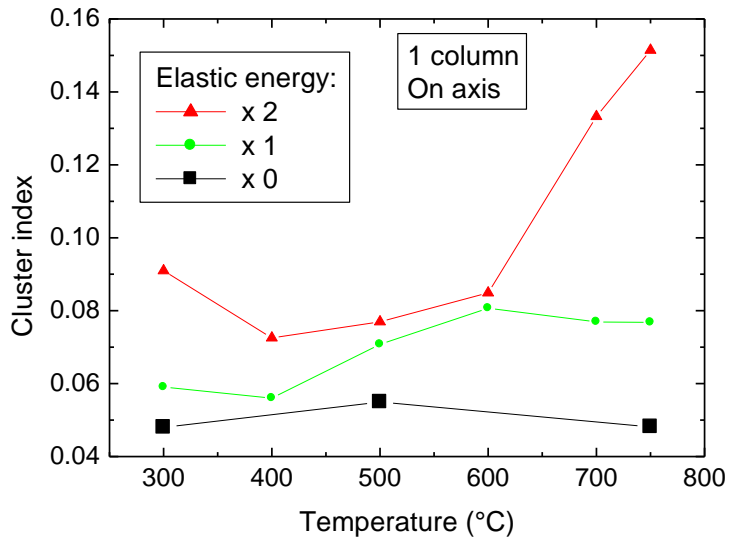


Figure 10: Cluster index for layers grown on on-axis substrate with 50% incident In, as a function of growth temperature. The index is calculated per atomic column. The energy related to the strain is set to double its value, or to its value, or to zero.